1998

Analysis of Stiction Effect on the Dynamics of Compressor Suction Valve

H. E. Khalifa
Carrier Corporation

X. Liu
Carrier Corporation

ANALYSIS OF A NEW TYPE COMPRESSOR

Takayoshi Fujiwara, Eiichi Aikawa, and Masayuki Okuda
Fuji Works, Toshiba Corporation
336, Tadewara, Fuji, Shizuoka, 416, Japan

ABSTRACT

A new type compression mechanism named ' Helical Blade Compressor' was presented at Purdue conference in 1992. There showed the design, performance of prototype , and theoretical analysis. Since then, fundamental experiment and theoretical analysis have clarified the phenomenon of the compression process. The gas is compressed in accordance with design theory of Helical Blade Compressor. This paper shows its potential by testing result of compression process against those of the other compression mechanism, rotary, screw, and scroll.

INTRODUCTION

Compressor evolution has moved from the reciprocating type to the rotary and scroll types, while the compression cycle has evolved from the intermittent process to continuous. The development has made a great contribution to achieving high efficiency. Especially, compression loss has decreased because continuous compression minimizes the pressure difference between the chambers, and non-valve mechanism. The Helical Blade Compressor is to be regarded as the successor compression mechanism which can realize even higher efficiency.

Structure and features

The Helical Blade Compressor is a unique compressor. Its main parts and the compression process are shown in Fig. 1 and Fig. 2.

This compression mechanism consists of 3 main parts, which is cylinder, rotor piston, and spiral blade. Rotor piston is a columnar part with a spiral groove on its outer surface. The pitch of spiral groove varies gradually from one end of rotor piston to the other. The spiral blade is made of elastic material, that can be easily set in the spiral groove at an uneven pitch. The rotor piston is located offset inside the cylinder, and the surface of rotor piston keeps in contact with the cylinder inner surface. Then the spiral blade divides the space between the cylinder and rotor piston into several compartments, each acting as a compression chamber.

While the rotor piston rotates inside the cylinder, that chamber moves in the axial direction. The volume of the chamber can be reduced from the suction side to the discharge side since the pitch of spiral groove decreases. The pressure in the chamber increases along the rotation.

This mechanism has three key features.

1. Low noise and low vibration due to a non-valve and continuous compression mechanism
2. High efficiency due to low leakage

3. smaller number of parts

EXPERIMENT RESULT AND ANALYSIS

Compression Volume and Pressure

The compression chamber of the Helical Blade Compressor is a space divided by a spiral blade, and is positioned between the rotor piston and cylinder. Supposing the compression volume is $V(\theta)$ at rotating angle θ, and polytropic compression takes place in the process, the pressure $P(\theta)$ is given by

$$P(\theta) = Ps \{ Vs / V(\theta) \}^n$$

where Ps is suction pressure, Vs is suction volume, and ' n ' is the polytropic coefficient.

As the volume $V(\theta)$ is decided by the form of the spiral blade, compression process varies by design. This point is the characteristic of the Helical Blade Compressor different from rotary and scroll mechanism.

Measurement of compression pressure

Measuring the practical pressure of each chamber is required to verify the gas is compressed according to the design. The result of the experiment reported in the paper are shown in the pressure versus angle diagram and pressure versus volume diagram.

The experiment model is shown at Fig. 3. The cylinder is fixed and rotor piston rotates inside cylinder. Several pressure sensors are attached to the cylinder along the spiral, every 270 degree from the suction side. Rotating position is monitored by the gap sensor. The disk attached to shaft has slit divided into 12, and the gap sensor faces it.

The data measured by the pressure sensor and gap sensor is memorized for calculation by a computer. The P-θ diagram is obtained when each of pressure datum is linked together. P-V diagram is obtained by transforming from angle θ to volume V.

Testing Result

First test results are shown in Fig. 4 and Fig. 5. Practical measurement results show that pressure in the chamber doesn't reach discharge pressure, and reverse flow occurs at the compression end. The design concept supposes that if the volume of chamber is the volume between rotor piston and cylinder, a fixed pressure ratio can be obtained. But measurement results differ from design concept.

If we then suppose the chamber volume is supplemented by the volume between blade and groove, the theoretical pressure curve is calculated as line (B) in Fig. 4. Measurement result is almost the same as line (B). Thus the volume of the compression chamber should be considered as the total volume of space V1 and V2.

$$P(\theta) = Ps \{ (Vs1+Vs2) / (V1(\theta)+ V2(\theta)) \}^n$$

where $V1(\theta)$ is the volume of space surrounded by cylinder and rotor piston, and $V2(\theta)$ is the volume of space surrounded by spiral blade and groove.

This experiment result that the space V1 and V2 is connected together leads the following idea. As shown Fig. 6, there should be a side clearance between the spiral blade and the spiral groove, and the spiral blade is attached to suction side surface of the groove during compression because of pressure difference. So the space V1 is connected with the space V2, and the gas is compressed as the same way.

Another experimental result of improved model is shown at Fig. 7 and Fig. 8, considering the former result. The gas is compressed according to fixed ratio of the new design. The theory of chamber volume is verified and confirmed by this diagram. P-V diagram based on P-θ diagram is shown at Fig. 8. From this diagram, it is known that there is hardly energy loss during suction and discharge process. It can be considered that non-valve mechanism prevents suction and discharge loss. And discharge passage area is secured enough to prevent gas pulsation loss.

Supposing the area surrounded by the measured pressure line and theoretical line is re-expansion loss, it is considered small. This shows less leakage between the chambers during compression because of less pressure difference, and it is characteristic feature of the Helical Blade Compressor.

CONCLUSION

From the experiment result, we may conclude the following.

1. The gas is compressed according to the design concept in the chamber of the Helical Blade Compressor.
2. The volume of compression chamber should be considered as the total volume of space of the rotor piston surface and spiral groove.

The design method of the Helical Blade Compressor has been established by noticing the chamber volume at this study. This paper shows the gas is compressed as design, and the compression process is flexibly changed according to spiral design variety. Spiral shape should be designed originally for high back use or low back use of each equipment. This suggests that Helical Blade Compressor can be applied for many refrigerating and air-conditioning system because of its flexibility and high potential.

REFERENCE

1. Hirayama, T., et al., "DEVELOPMENT OF A NEW COMPRESSION MECHANISM", Proc. of the 1992 int. Compressor Eng. Conf. At Purdue, July 1992, pp. 21-30.

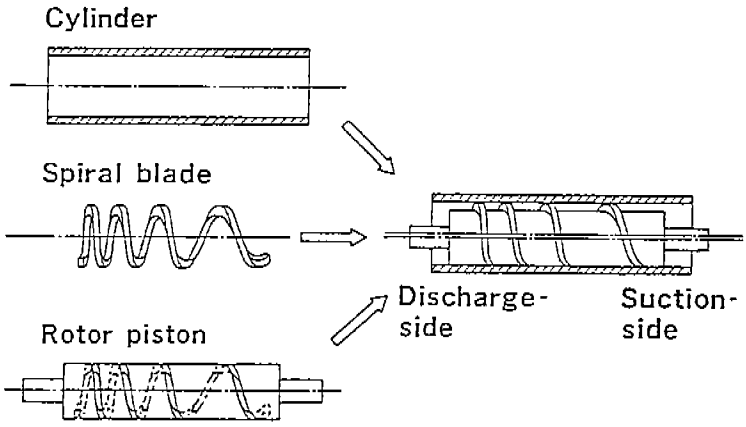

Fig. 1 Three Main Parts

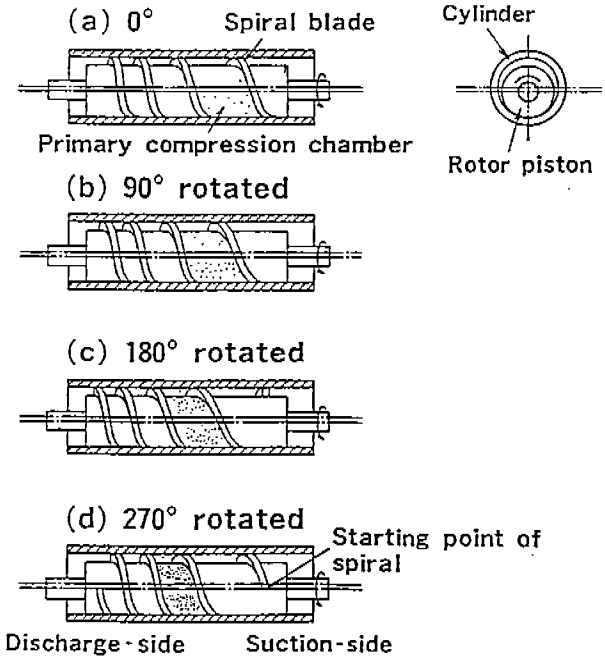

Fig. 2 Compression Process

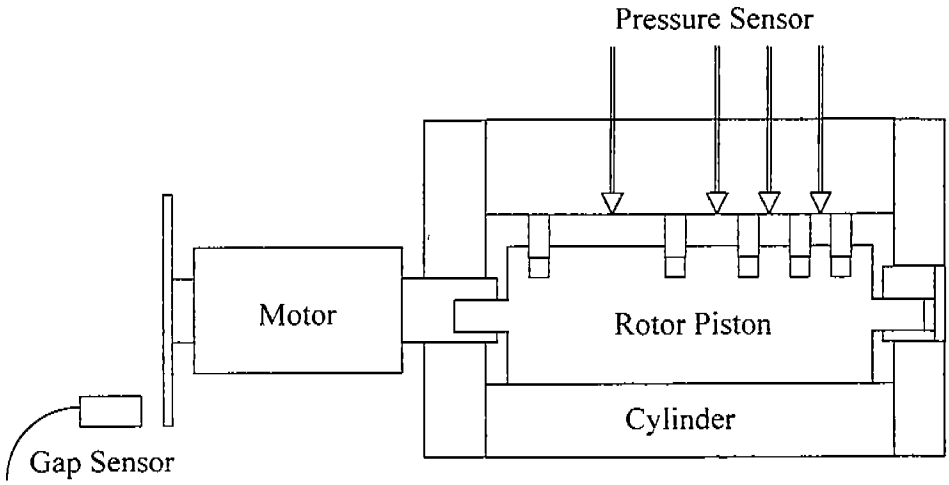

Fig.3 Measuring Model

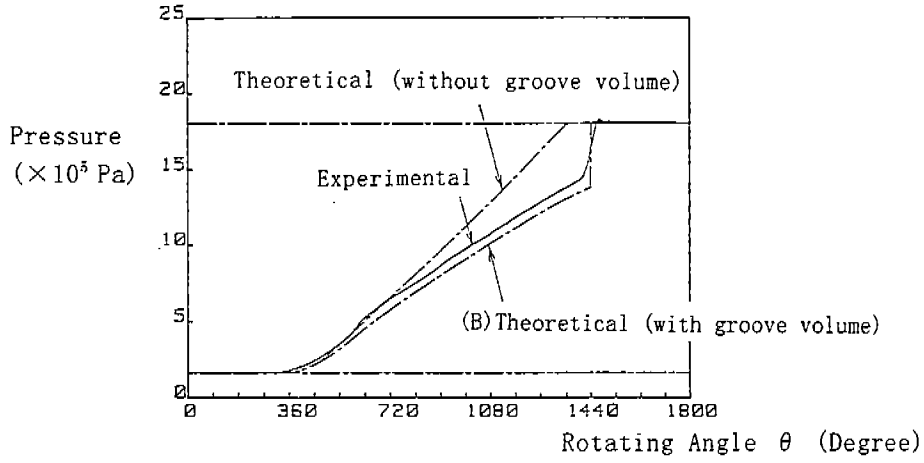

Fig.4 P-θ diagram -(1)

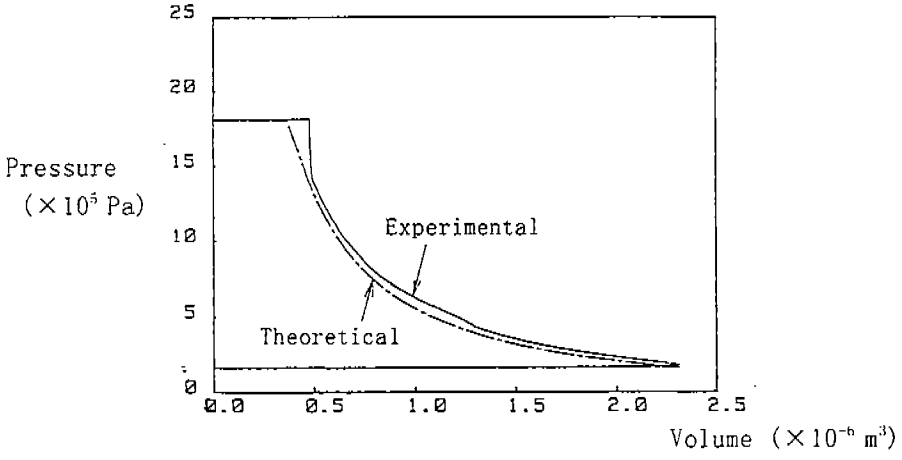

Fig.5 P-V Diagram -(1)

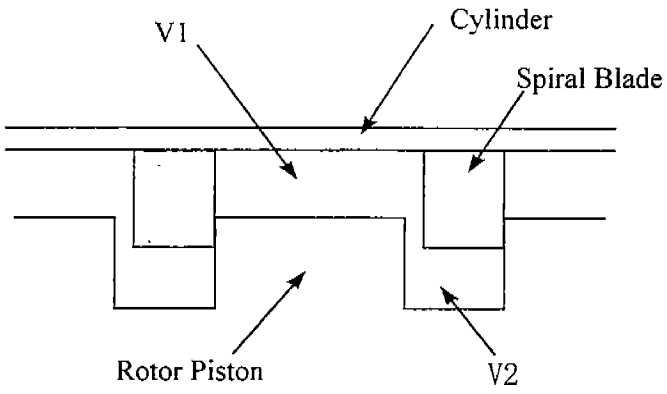

Fig.6 Compression Chamber

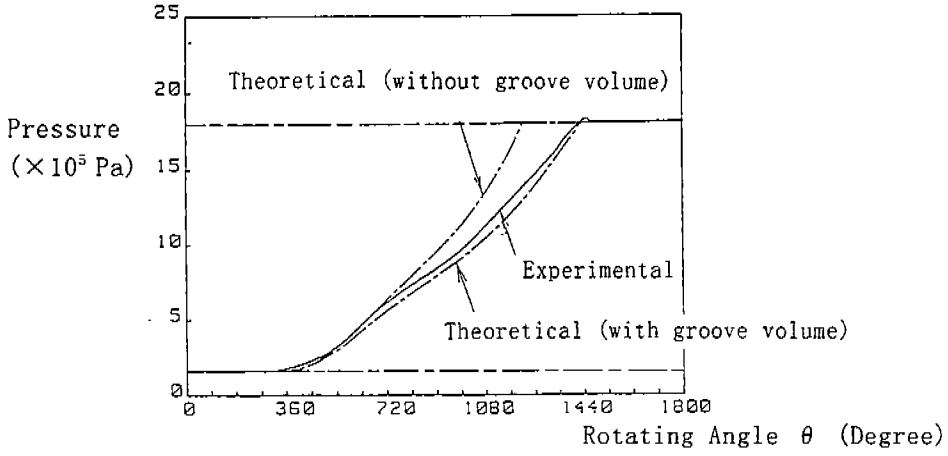

Fig.7 P-θ diagram -(2)

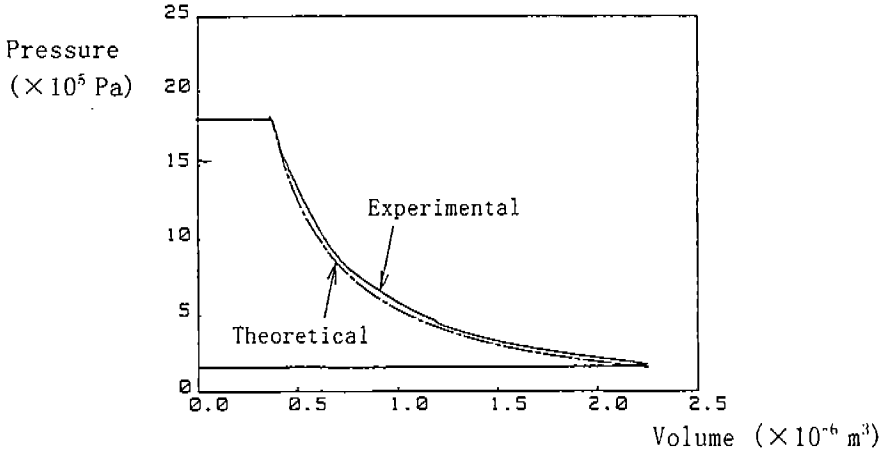

Fig.8 P-V Diagram -(2)

ANALYSIS OF STICTION EFFECT ON THE DYNAMICS OF COMPRESSOR SUCTION VALVE

H. Ezzat Khalifa and Xin Liu

Carlyle Compressor Division
Carrier Corporation
6500 Chrysler Drive
Syracuse, NY 13221

ABSTRACT

An analytical model is presented for analyzing the dynamic behavior of a round reed valve in the presence of oil. It is shown that the primary reason for stiction is the viscous force arising from dilating the oil film between the valve and its seat. The relative effect of oil viscosity and valve/seat contact area on valve force is presented for a representative reciprocating compressor.

INTRODUCTION

Oil films between the suction valve and its seat in reciprocating compressors have been shown to cause the valves to adhere to their seats and open much later than they would have without the presence of oil [Wambsganss *et al.*, 1967, MacLaren and Kerr, 1969, Brown *et al.*, 1975, and Giacomelli and Giorgetti, 1974]. This phenomenon is known as valve stiction and has been studied both analytically and experimentally [MacLaren *et al.*, 1969, Brown *et al.*, 1975, Giacomelli and Giorgetti, 1974, Pringle, 1976, Bauer, 1990, and Prasad and Panayil, 1996]. The simplest approach to accounting for this phenomenon was to introduce a time delay in the valve dynamic model [MacLaren *et al.*, 1969, and Brown *et al*, 1975]. More sophisticated models provided solutions of the thin-film, low Reynolds-number Navier-Stokes equations for simple valve geometries subjected to time-varying pressure differences [Pringle, 1976]. The physical situation is the opposite of the squeeze film effect well known in lubrication theory [Booker, 1983]. Attempts have also been made at including the effect of cavitation on film rupture to account for the liberation of dissolved gases (e. g., refrigerant) when the pressure in the film interior drops as a result of film dilation [Pringle, 1976, and Khalifa and Liu, 1997]. The rapid release of the valve and the associated impact are shown to subject the valve to much higher forces than would be experienced without the effect of stiction. Valve stress could be reduced by reducing the contact area between the valve and its seat [Fraser *et al.*, 1997]. The present paper primarily focus on the effect of oil on suction valve dynamics in reciprocating compressor.

NOMENCLATURE

a, A	Area [m^2]
c	Damping coefficient [N.s/m]
d	Damping factor
F	Force [N]
G	Mass flow per unit area
h	Film thickness [m]
k	Spring stiffness [N/m]
L	Connecting rod length
m	Effective valve mass [kg]
M	Gas mass in cylinder [kg]
n	Polytropic exponent
P	Pressure [Pa]
Q	Volume flow rate [m^3/s]
r, R	Radius [m]
S	Stroke [m]
t	Time [s]
u	Radial velocity [m/s]
V	Cylinder volume [m^3]
w	Axial (normal) velocity [m/s]
z	Axial coordinate in cylindrical coordinates

Greek Letters:

α	Clearance volume/swept volume
β	Meniscus contact angle [rad]
γ	Isentropic exponent
λ	L/S ratio
μ	Dynamic viscosity [Pa.s]
ρ	Density [kg/m^3]
σ	Surface tension [N/m]
Ω	Angular velocity [rad/s]
ξ	Dimensionless radial distance

Subscripts and Superscripts

c	Contact; cylinder; critical
d	Discharge
g	Gas
i	Inner
o	Outer
p	Port
s	Suction; spring
t	Tension (surface)
v	Viscous

VALVE MODEL

The model employed in this analysis is a simplified configuration that captures the important physics while keeping the analysis to a tractable level. As illustrated in Figure 1, the valve system is simulated as a rigid round disc of radius R_o and mass m, operating in conjunction with a concentric round port of radius R_i. The valve disc is supported on a two-stage spring with stiffness k_1 and k_2 and is constrained to move only in the axial direction against the spring. The spring stiffnesses are selected to represent a reed valve that opens initially as a cantilever with a stiffness k_1 until its free tip rests against a stop at a distance $z=h_s$ from the closed position ($z = 0$), at which point, the reed deflects as a simple beam with a stiffness k_2. In this fashion the valve deflects in a stepwise nonlinear fashion according to:

$$k = k_1 \quad \text{for } h \le h_s,$$
$$k = k_2 \quad \text{for } h > h_s. \tag{1}$$

It is assumed that there is an oil film between the valve and the valve seat, replenished by oil carryover into the suction port. The cylinder end of the film is terminated as a meniscus separating the oil film from the cylinder gas. The pressure in the port is assumed to be constant and equal to the suction pressure P_s. The pressure of the cylinder, P_c, varies in accordance with piston movement , and gas flow when the valve opens.

Valve dynamics can be divided into two stages, before and after the rupture of the oil film. Before the rupture of the oil film, valve dynamics is strongly influenced by the viscous flow of the oil or the oil/refrigerant mixture in the dilating film between the valve and its seat. After the rupture of the oil film, the viscous and capillary forces can be removed from the force balance, and valve dynamics can be simulated by a typical second order dynamic system. In the following sections, the behavior of valve dynamics in these two stages will be discussed.

OIL FILM MECHANICS

At low Reynolds numbers in thin films, the Navier-Stokes equations reduce to the Reynolds equations of hydrodynamic lubrication [Brooker, 1983],

$$\frac{\partial P}{\partial r} = \mu \frac{\partial^2 u}{\partial z^2}, \tag{2}$$

whose integration for thin films is a parabolic radial velocity distribution across the film,

$$u = \frac{1}{2\mu}\frac{dP}{dr} z(z-h). \tag{3}$$

The radial flow between the valve and its seat at any radius r is given by the integration of the parabolic velocity profile (Eq. 3) across the oil film from $z = 0$ to $z = h$:

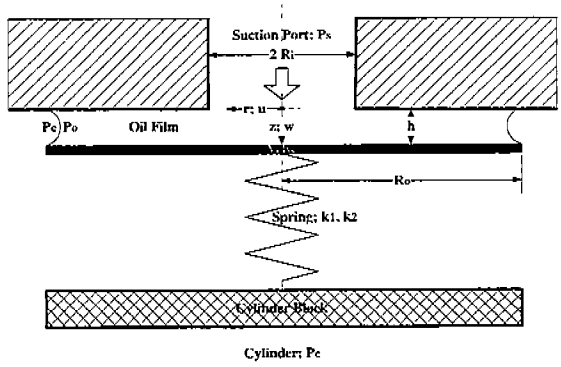

Figure 1 Suction Valve Geometry

$$Q(r) = -\frac{\pi r}{6\mu}\frac{dP}{dr}h^3. \tag{4}$$

From the continuity equation, the flow $Q(r)$ should also satisfy the equation

$$Q(r) = -\pi\left(r^2 - R_i^2\right)\frac{dh}{dt} + Q(R_i), \tag{5}$$

with $dh/dt = w$ representing the valve axial velocity. Equating (4) and (5), we obtain

$$r\frac{dP}{dr} = \frac{6\mu}{h^3}\frac{dh}{dt}\left(r^2 - R_i^2\right) - R_i\left(\frac{dP}{dr}\right)_{R_i}. \tag{6}$$

Let the normalized radius $r/R_i = \xi$ and $R_o/R_i = X$, then Eq. (6) can be recast in the form:

$$\frac{dP}{d\xi} = \frac{6\mu}{h^3\xi}\frac{dh}{dt}R_i^2\left(\xi^2 - 1\right) + \frac{1}{\xi}\left[\frac{dP}{d\xi}\right]_X, \tag{7}$$

whose integration with respect to ξ is:

$$P = \frac{3\mu}{h^3}\frac{dh}{dt}R_i^2\left(\xi^2 - 2\ln\xi\right) + \ln\xi\left(\frac{dP}{d\xi}\right)_X + C \tag{8}$$

The boundary conditions $P = P_s$ at $\xi = 1$ and $P = P_o$ at $\xi = X$ establish the values of C and $(dP/d\xi)_i$ as follows:

$$C = P_s - \frac{3\mu}{h^3}\frac{dh}{dt}R_i^2, \tag{9a}$$

$$\left(\frac{dP}{d\xi}\right)_X = \frac{1}{\ln X}\left[-(P_s - P_o) + \frac{3\mu}{h^3}\frac{dh}{dt}R_i^2\left(1 - X^2 + 2\ln X\right)\right] \quad (9b)$$

which lead to the following equation for the pressure distribution in the film

$$P - P_o = (P_s - P_o)\left(1 - \frac{\ln\xi}{\ln X}\right) + \frac{3\mu}{\pi\ h^3}\frac{dh}{dt}R_i^2\left[\xi^2 - 1 + \frac{\ln\xi}{\ln X}\left(1 - X^2\right)\right] \quad (10)$$

The existence of a meniscus at the outer rim causes the pressure inside the film to differ from that of the cylinder gas,

$$P_o - P_c = \frac{-2\sigma\cos\beta}{h} \quad (11)$$

which can be substituted in Eq. (10) to eliminate the film interior pressure at the meniscus, P_o, in favor of the cylinder pressure, P_c:

$$P - P_c = (P_s - P_o)\left(1 - \frac{\ln\xi}{\ln X}\right) - \frac{2\sigma\cos\beta}{h} + \frac{3\mu}{\pi\ h^3}\frac{dh}{dt}R_i^2\left[\xi^2 - 1 + \frac{\ln\xi}{\ln X}\left(1 - X^2\right)\right] \quad (11b)$$

The total force introduced by the oil viscosity is the integration of the above pressure over the area covered by the oil film, which is

$$F_v = \int_{R_i}^{R_o} 2\pi\ r P dr = \int_1^X 2\pi\ R_i^2\ \xi\ \ P d\xi = \pi\ R_i^2\left[X^2 P_c - P_x - \frac{\left(X^2 - 1\right)\left(P_c - P_s\right)}{2\ln X}\right] - \pi\ R_i^2\left(X^2 - 1\right)\frac{2\sigma\cos\beta}{h} + \frac{3\pi\ \mu}{2h^3}\frac{dh}{dt}R_i^4\left(1 - X^4 + \frac{1 - 2X^2 + X^4}{\ln X}\right) \quad (12)$$

The first term on the RHS of Eq. (12) , in addition to the pressure difference in the port area, gives rise to a gas force, F_g, on the valve due to the pressure difference between suction and cylinder pressures. This force vanishes if that pressure difference is zero. The second term gives rise to a surface tension force, F_t; it vanishes if there is no meniscus at the valve outer rim. The last term gives rise to a viscous force, F_v, which vanishes if the viscosity is zero, if the valve is stationary ($dh/dt = 0$) or if the contact area is zero ($\xi = X = 1$). These forces are derived by integrating the pressure distribution over the entire valve area, i. e., from $\xi = 0$ to $\xi = X$, noting that only the pressure difference force is present from $\xi = 0$ to $\xi = 1$. Therefore,

$$F_g = \pi R_i^2 (P_s - P_c)\left[\frac{(X^2 - 1)}{2\ln X}\right], \quad (13)$$

$$F_t = -\pi R_i^2\left(X^2 - 1\right)\frac{2\sigma\cos\beta}{h}, \quad (14)$$

$$F_v = +\frac{3\pi\ \mu}{2h^3}\frac{dh}{dt}R_i^4\left(1 - X^4 + \frac{1 - 2X^2 + X^4}{\ln X}\right). \quad (15)$$

We note that the terms in the brackets are purely geometrical and depend only on the ratio of the contact area to that of the port ($X^2 = 1 + A_c/A_p$). The presence of h^3 in the denominator of the viscous force (Eq. 15) causes this force to decrease rapidly as the film is dilated under the action of the gas force when P_c is lower than P_s.

VALVE OPENING PROCESS

The equation of motion of the valve in the presence of the oil film is given by:

$$m\frac{d^2h}{dt^2} - F_v + kh = F_g + F_t, \quad (16)$$

in which k is given by Eq. (1). Equation (16) is highly nonlinear and can be solved numerically. Before attempting that, we need to assess the relative magnitude of the various terms in Eq. (16) and how this is affected by h. In doing so, we note that the second term in Eq. (16) could be put in the traditional damping form:

$$-F_v = \Phi_v\frac{3\pi\mu}{2h^3}R_i^2\frac{dh}{dt} = c\frac{dh}{dt}, \quad (17)$$

where Φ_v is the geometrical function of X in the curly brackets of Eq. (15) and c is equivalent to the traditional damping coefficient in a spring-mass system[1], except that it is a strong function of h in this case.

The cylinder pressure can be explicitly determined as a function of time (crank angle) from the variation of pressure inside the closed cylinder during the clearance gas re-expansion process, assumed here to be polytropic with a known exponent n. Specifically, for a piston/connecting rod/crank mechanism we may write:

[1] Without loss of generality, the surface tension term will be ignored in the analogy with the damped spring-mass system. It will be shown later that unless $h << 1$ μm, F_t could be safely neglected.

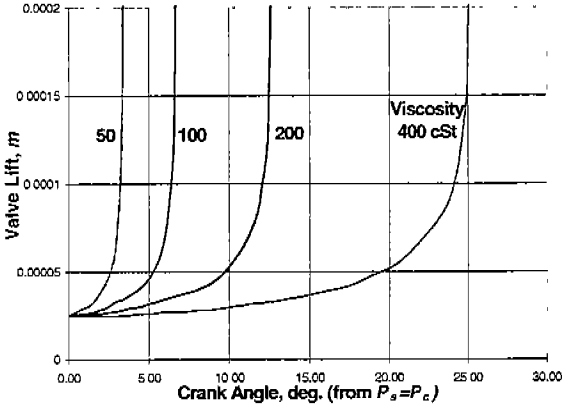

Figure 2 Effect of Oil Viscosity on Valve Timing

$$\frac{P_c}{P_s} = \frac{P_d}{P_s}\left[1+\frac{1}{\alpha}\left(\lambda+\frac{1}{2}(1-\cos\theta)-\sqrt{\lambda^2-\frac{1}{4}\sin^2\theta}\right)\right]^{-n} \tag{18}$$

This pressure will act on the valve disc forcing it to move away from the valve. The model presented so far allows us to determine the effect of oil on valve timing. Figure 2 depicts the effect of oil film viscosity on suction valve timing as computed from a numerical solution of Eq. (17). All cases correspond to an initial film thickness of 0.001 inch (~25 μm), pressure ratio of 2.5 and a suction pressure of 0.2 MPa (~29 psia). The end of each curve is arbitrarily selected to coincide with the point at which the damping factor falls below 5. The strong influence of oil film viscosity on valve timing is clearly evident.

These equations were employed to calculate valve lift and velocity for a typical R404A compressor case. Figure 3 depicts the suction valve lift and velocity over the entire suction stroke when the oil viscosity at the valve is 400 cSt. A lower initial film thickness will increase the viscous force and delay valve timing and vice versa.

Figure 4 presents the pressure distribution inside the oil film at several crank angles during film dilation μ = 400 cSt. It can be seen that the pressure drops well below the cylinder pressure over a significant portion of the contact area, which gives rise to a force that resists valve opening. It should be noted that such depression in film pressure could only proceed so long as cavitation does not take place. The onset of cavitation in refrigerant-saturated oil will accelerate film rupture and cause the valve to lift more quickly. Cavitation effects in oil films are addressed in Pringle's thesis [1976].

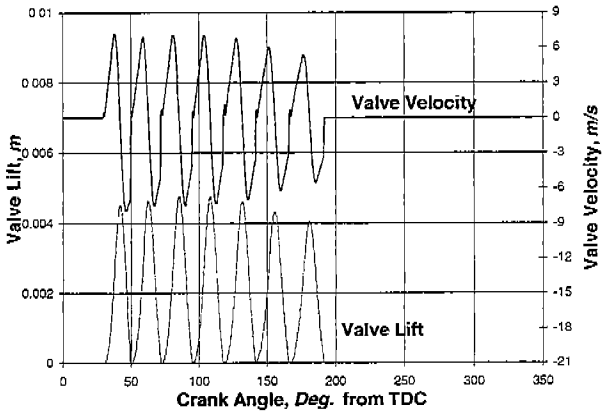

Figure 3 Valve Opening Dynamics

VALVE DYNAMICS

Valve dynamics after film rupture and cylinder pressure are inter-related and can be obtained also from a numerical solution of Eq. (16). The gas force in this phase of valve lift must be determined from cylinder pressure, which will no longer vary in accordance with Eq. (18), but will depend on the cylinder filling process. A compression chamber can be considered as a control volume with a moving boundary.

Thermodynamic properties, u, and h can be determined from a pair of intensive properties, say p and T. Any mass flow, heat flow, or work flow will make the process deviate from the isentropic process.

For the geometry of Figure 1, the valve throat area is given by:

$$\begin{aligned} a &= 2\pi h R_i \quad \text{for } h < \frac{A_p}{2\pi R_i} \\ a &= A_p \quad \text{for } h \geq \frac{A_p}{2\pi R_i} \end{aligned} \tag{19}$$

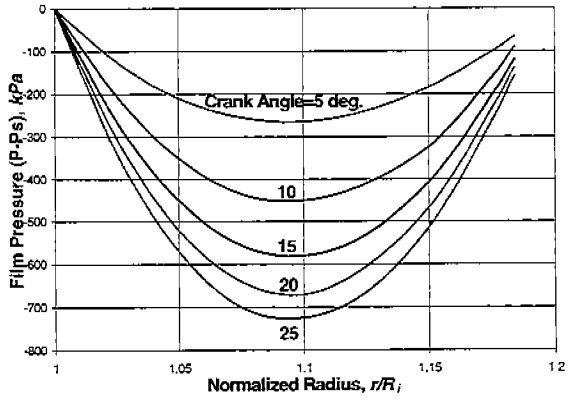

Figure 4 Oil Film Pressure Distribution

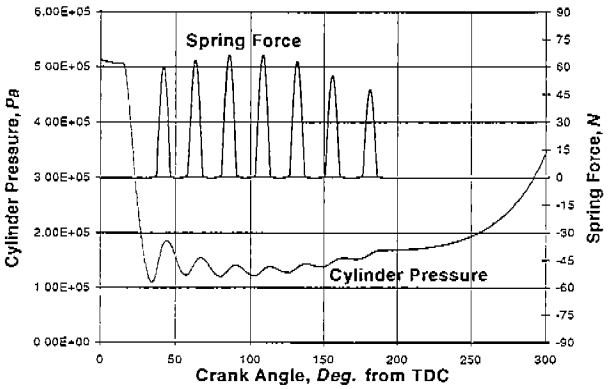

Figure 5 Cylinder Pressure and Spring Force

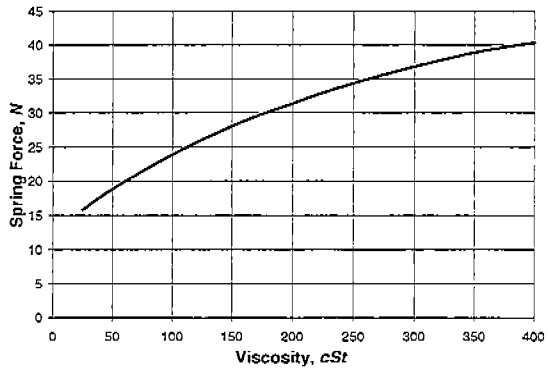

Figure 6 Effect of Film Viscosity on Spring Force

The flow in the valve passage is a complex two-phase compressible flow of refrigerant and oil. For the purposes of this analysis, the effect of oil will be ignored and this complex flow will be approximated as a polytropic compressible flow of a perfect gas through a variable area-conduit. The mass flow per unit area at any given section of this conduit is given by:

$$\dot{m} = C_d \sqrt{\frac{2n}{n-1} P_s \rho_s \left(\frac{P}{P_s}\right)^{2/n} \left[1 - \left(\frac{P}{P_s}\right)^{(n-1)/n}\right]} \qquad (20)$$

in which C_d is an empirical discharge coefficient and P is the pressure at the flow section where $\dot{m}$ is evaluated. For choked flow, this reduces to

$$\dot{m}^* = C_d \sqrt{n P_s \rho_s} \left(\frac{2}{n+1}\right)^{\frac{n+1}{2(n-1)}}, \qquad (21)$$

with $\dot{m}^*$ representing the critical mass flow per unit throat area. Equation (20) also serves as a relationship for computing the pressure distribution as a function of ξ (flow area). This set of equations can be readily accommodated in the numerical integration of Eq. (16), with the gas force during the cylinder filling process given at any given instant of time by the integration of $P(\xi)$-P_c over the valve area, including any area extension beyond the stiction zone, over which the pressure of the flowing gas may be different from the cylinder pressure, giving rise to an additional gas force on the valve. The initial film thickness in this case was assumed to be 25 μm (0.001 in). It can be seen (Figure 4) that the valve bounces on its seat and oscillates several times before it finally closes a little beyond BDC[2]. It can also be seen that the highest velocity (7.5 m/s) in its first opening cycle beginning. This is nearly 30° of delay from the ideal suction valve opening crank angle[3].

Figure 5 shows the cylinder pressure and valve spring force associated with the same case The spring force is a measure of valve stress. A pronounced under-pressure develops in the cylinder before the valve begins to open. This under-pressure, coupled with the high velocity of the valve when it impacts its stop result in a sharp increase in valve stress compared with the a no- or low-stiction case. This is illustrated in Figure 6, which compares spring force in the first opening cycle for the same configuration as a function of film viscosity. Figures 7 show that the spring force could be substantially reduced by lowering the viscosity or reducing the contact area. This is in full accord with observed experimental behavior of AB/R22 (μ ~ 100 cSt) and POE/R404A (μ ~ 1000 cSt) in low temperature

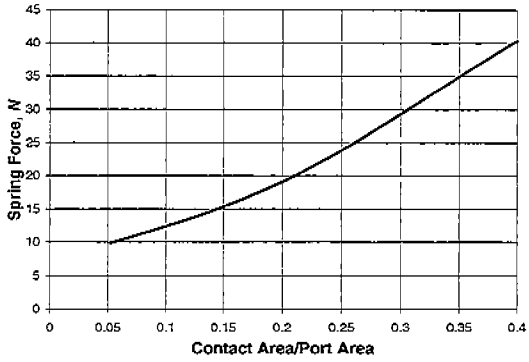

Figure 7 Effect of Contact Area on Spring Force

[2] In the presence of dissolved refrigerant, the film pressure will fall until the onset of cavitation and the formation of a vapor bubbles. The vapor zone will be at a more or less constant pressure, and the viscous stiction force will be diminished as a result [5].

[3] The ideal suction valve opening angle is that at which the cylinder pressure drops below suction pressure. Its value depends on the pressure ratio, clearance ratio and re-expansion exponent.

refrigeration applications (at ~ -40 °C saturation temperature).

The so-called valve stiction phenomenon in reciprocating compressors can be fairly well represented by a simple model of viscous oil film dilation and the film pressure depression resulting from it. Should the film terminate at the valve edge in a concave meniscus, surface tension could contribute to the film pressure depression. However, the contribution is negligible in comparison with that of viscous dilation in films that are likely to occur in practice. The present model does not take film cavitation [Khalifa and Liu, 1997] into account. Film cavitation accelerates film rupture and the non-uniformity of oil carryover to the valve makes the stiction phenomenon rather erratic. Nontheless, valve behaveior in the presence of oil can be well estimated and predicted by this model and the relative effect of the various design and operating parameters can be derived from it.

CONCLUDING REMARKS

The present model assumes that sufficient oil is present at the valve, specifically between the valve and its seat. In an operating compressor, this may not always be the case, as the presence of oil at the valve will depend on the oil management arrangement in the system and within the compressor. Furthermore, the viscosity of the oil at the valve will not remain constant from stroke to stroke and during the same stroke because of heat transfer and the unsteady concentration of refrigerant in the oil. The oil that reaches the valve is a non-uniform mixture of oil from the compressor crankcase, oil returned from the system and residual oil inside the cylinder, all of which have varying concentrations of dissolved refrigerant and each having a different temperature.

ACKNOWLEDGEMENTS

The authors are grateful to Dr. Harvey Michels of United Technologies Research Center, who provided the viscosity data of the POE/R404A system at low temperatures. They are also grateful to Messers Bruce Fraser, Michael Dormer, Wayne Beagle, Peter Kaido and Kyle Wessels, all of the Carrier Carlyle Compressor Division, who provided the compressor characteristics used in this model.

REFERENCES

Batchelor, G. K., *An Introduction to Fluid Dynamics*, Cambridge University Press, London, 1970.

Bauer, F., 1990, "The Influence of Liquid on Compressor Valve, " Proceedings of 1990 International Compressor Engineering Conference at Purdue, Vol.2, pp.647-653.

Booker, J. F., "Squeeze Films and Bearing Dynamics", *Handbook of Lubrication*, CRC Press, Boca Raton, 1983.

Brown, J., Lough, A., Pringle, S. and Karll, B., "Oil Stiction in Automatic Compressor Valves", IIR Congress, Moscow, 1975.

Fraser, B.A., Kaido, P.F., and Dormer, M.J., 1997, Enhanced Oil Film Dilation for Compressor Suction Valve Stress Reduction, U.S. patent serial No. 80/868,790, June 4, 1997.

Giacomelli, E. and Giorgetti, M., "Investigation on Oil Stiction in Ring Valves", Proc. Purdue Compressor Technology Conference, 1974.

Israelachvili, J., *Intermolecular and Surface Forces*, 2nd Ed., Academic Press, London, 1991.

Khalifa, H.E. and Liu, X., "Opening Mechanism of Compressor Valve in the Presence of Oil," Proceedings of the 2nd International Compressor Technique Conference, August 16-18, Chengdu, China, 1997.

MacLaren, J. F. T. and Kerr, S. V., "Automatic Reed Valves in Hermetic Compressors", IIR Commission III, Prague, 1969.

Prasad, B.G.S. and Panayil, D., "Valve Stitction in Reciprocating Compressors," Proceedings of the ASME Advanced Energy Systems Division, AES-Vol. 36, pp.171-180, 1996.

Pringle S., "Oil Stiction in Automatic Compressor Valves", Ph.D. Thesis, University of Strathclyde, Scotland, 1976.

Wambsganss, W. M. and Cohen, R., "Dynamics of a reciprocating Compressor with Automatic Reed Valves", Proc. XII Int. Congr. Refrig. Madrid, 1967.